

Original Research Article

Hydroxyherderite as a novel filler for a dental adhesive

ABSTRACT

Aims: The aim of this study was to incorporate Hydroxylherderite (HEr) into an adhesive and evaluate the properties of the resulting material.

Study design: *In vitro* study.

Methodology: Hydroxylherderite was incorporated into the adhesive at concentrations of 2% and 5% by weight. The degree of conversion (DC, $n = 3$) was measured using an ATR-FTIR spectrometer. After immersion in absolute ethanol for two hours, the softening of the adhesive was assessed using a microhardness tester with a Knoop indenter. After 7 and 28 days of immersion in Simulated Body Fluid (SBF), mineral deposition in the adhesive was evaluated using a Raman microscope. Cell viability in contact with the adhesive was assessed according to ISO 10993-5. Data were analyzed using paired t-tests, ANOVA, and Tukey's post hoc tests with a significance level set at 0.05.

Results: The incorporation of HEr into the adhesive did not affect the degree of conversion compared to the control. DC ranged from $59.21 \pm 11.11\%$ to $63.49 \pm 5.30\%$. The 5 wt% group showed a significant increase in initial microhardness ($p < 0.05$). Higher mineral deposition was observed with increased immersion time HEr concentration. All HEr concentrations maintained cell viability above 80% after 48 and 72 hours of contact.

Conclusion: HEr was successfully incorporated into the adhesive resin, promoting mineral deposition without cytotoxic effects and without compromising the physicochemical properties of adhesive.

Keywords: Adhesives. Biomimetics. Biotechnology. Operative Dentistry.

1. INTRODUCTION

The bonding mechanism results from demineralization, resin infiltration, and polymerization, leading to micromechanical interlocking in the enamel etch-pits and exposed collagen in dentin¹⁻³. Discrepancies in etching depth and monomer infiltration and degradation of polymer matrix could leave denuded collagen in hybrid layer. The presence of denuded organic fibrils, along with residual solvent from the adhesive system and aqueous fluid in dentinal tubules, can compromise adhesion performance^{1,2}. Consequently, adhesion becomes vulnerable to hydrolytic degradation, which breaks covalent bonds in the polymer³, and collagen biodegradation due to enzyme activation in the acidic environment of dentin^{2,4}.

To address these limitations, several inorganic fillers have been incorporated into adhesive materials, improving their properties and the longevity of adhesion. Among these are hydroxyapatite⁵, calcium phosphates⁶, zinc oxide⁷, bioactive glasses⁸. Inorganic fillers replace part of the organic polymeric matrix, which decreases both hydrolytic^{2,4} and

enzymatic degradation⁹, while promoting interaction with biological tissues¹⁰. The ion release from adhesives containing bioactive particles promotes mineral deposition, thereby protecting dentin collagen^{11,12}. Dentin biomineralization requires ion precipitation in both the intrafibrillar and interfibrillar spaces of collagen. These spaces correspond to the gap zone of collagen fibrils and the surface of collagen fibrils, respectively. Proposed mechanisms for dentin mineralization can be based on classical ion-cluster theories or non-classical amorphous precursor theories. Intrafibrillar mineralization also includes mechanisms such as polymer-induced liquid precursor, which enables minerals to be drawn into the gaps of collagen fibrils through capillary infiltration. Furthermore, electrostatic attraction between the positive charges near the C-terminal end of collagen molecules and ions facilitates infiltration into collagen fibrils. The collagen framework serves as a site for mineral deposition, acts as a gatekeeper for various molecules, and regulates diffusion into the inner spaces of collagen fibrils. Theories of interfacial energy-guided mineralization and Gibbs-Donnan equilibrium must be established between the extrafibrillar and intrafibrillar spaces of collagen fibrils, balancing electrostatic neutrality and osmotic equilibrium. Consequently, improving the mechanical, chemical, and biological properties of the adhesive and hybrid layer can extend the clinical longevity of adhesion.

Beryllium (Be) is found on the Earth's surface at an average concentration of 3 ppm¹³. This mineral exhibits high hardness and dimensional stability under a wide range of temperatures^{13,14,15}. Beryllium compounds are widely distributed and can be found in many countries, including Brazil^{13,15}. The stability and reaction between beryllium (Be), calcium (Ca), and phosphate (PO₄) result in hydroxylherderite (HEr)^{13,14,15}. This compound has a monoclinic structure, consisting of sheets of corner-sharing phosphate units and BeO₃OH tetrahedra, linked along the c-axis by sheets of edge-sharing Ca-containing polyhedra, as described in previous crystallographic studies on hydroxylherderite from Minas Gerais, Brazil¹⁶. In addition to its favorable mechanical properties, the beryllium-modified calcium phosphate compound also demonstrates biological potential. The precipitation efficiency of calcium phosphate is significantly affected by the Ca/P ratio¹⁷. The Ca/P ratio of HEr is 1.2918, which is close to the desirable value of 1 and similar to the ratios of enamel (1.59), dentin (1.67), octacalcium phosphate (OCP, 1.33), tricalcium phosphate (TCP, 1.5) and hydroxyapatite (HA, 1.67). When the ratio is closer to 1.67, the resulting material exhibits lower solubility. Although HA is considered the most stable compound with superior mechanical properties compared to others, it still falls short in some areas due to its hydrophilicity and porosity¹⁹. Therefore, hydroxylherderite can serve as an alternative to previously used calcium phosphate compounds in the search for a material that not only enhances physical and mechanical properties but also maintains its biological potential. However, no reports exist on the incorporation of HEr in dental adhesive. The aim of this study was to incorporate HEr into an adhesive and evaluate the properties of the resulting material.

2. MATERIAL AND METHODS

2.1 Hydroxylherderite process and characterization

Samples of Hydroxylherderite (CaBe[PO₄]OH) were collected from different pegmatites in Minas Gerais, Brazil. The mineral was pulverized in an agate mortar, resulting in particles with an average size of 5 μm. The samples were analyzed by powder X-ray diffraction using a D8 Advance DaVinci diffractometer with CuK radiation. Chemical characterization of hydroxylherderite was performed by Electron Microprobe Analysis (EMP). The sample was analyzed at five distinct spots using a Jeol JXA8900R spectrometer. The standards for each element included Ca–Apatite, P–Ca₂P₂O₇, F–Fluorite, Mn–Rhodonite, Fe–Magnetite, Al–Al₂O₃ and Mg–MgO. Stoichiometric calculations were used to determine the quantities of Be and H₂O. A thin layer of evaporated carbon was applied to the hydroxylherderite samples. The electron

probe microanalysis in WDS (wavelength dispersive spectrometer) mode was conducted at a 15 kV accelerating voltage and a beam current of 10 nA. The results were averaged from five spots.

2.2 Incorporation of Hydroxylherderite into adhesive

The Hydroxylherderite (HEr) was incorporated into a commercial adhesive (Scotchbond MP, 3M-ESPE, St Paul, Minnesota, USA) at 2% and 5% by weight. An adhesive with no particles was used as the control group. The monomer composition of this commercial adhesive is Bisphenol A Diglycidyl Ether Dimethacrylate (BISGMA; 55-65 wt%) and 2-Hydroxyethyl Methacrylate (HEMA; 35-45 wt%), as reported by the manufacturer. The incorporation of HEr into the adhesive was achieved by mixing and ultrasonication (CBU 100/1 LDG, Plana, São Paulo, SP, Brazil) for 30 minutes.

2.3 Degree of conversion (DC)

The degree of conversion of adhesives (HEr 0%, 2%, 5%) was determined using an attenuated total reflectance (ATR) device of a Fourier-transform infrared (FTIR) spectrometer (Vertex 70, BrukerOptics, Ettlingen, Alemanha). A disk (3.0 mm diameter and 2.0 mm thickness) from each adhesive ($n = 3$) was photoactivated for 20 seconds by a light-emitting diode (LED) with 1,200 mW/cm² irradiance (Radii cal, SDI, Bayswater, Baden-Württemberg, Austrália). Before and immediately after photoactivation, absorbance spectra (32 scans, 4 cm⁻¹ resolution) were obtained. The degree of conversion was calculated based on the peak height (intensity of absorbance) of the aliphatic carbon-carbon double bond stretching vibration at 1638 cm⁻¹ and aromatic ring at 1608 cm⁻¹.

2.4 Softening in ethanol

Disk samples (5.0 mm diameter and 1.5 mm thickness; $n = 3$) were prepared, embedded in acrylic resin, and polished with a series of silicon carbide (SiC) papers (600, 1200, and 2000 grit) for 2 minutes each. Microhardness was evaluated using a Knoop indenter at a load of 25 g for 15 seconds in a microhardness tester, before (initial) and after immersion (final) in absolute ethanol and water (1:1, 200mL) for 2 hours. The percentage reduction in microhardness was calculated. Three indentations were made on each sample surface.

2.5 Mineral deposition

Mineral deposition was analyzed using a Raman InVia microscope (Renishaw, Wotton-under-Edge, Gloucestershire, United Kingdom). Three disks from each group were used. Each sample was immersed in 15 ml of Simulated Body Fluid (SBF) for 7 and 28 days at 37 °C. The Simulated Body Fluid (SBF) was formulated according to ISO 23317. The center of each sample (area of 10 × 10 μm) was irradiated by a helium-neon laser (785 nm). Spectra were obtained from 440 to 1800 cm⁻¹ before and after immersion in SBF (7 and 28 days). Images were processed using WiRe software 5.2 (Renishaw). The peak height at 960 cm⁻¹, corresponding to the phosphate content⁵, was used for analysis. To map the chemical changes on the surface of the samples, the average intensity of the phosphate peak was calculated from the three samples.

2.6 Cytotoxicity

Cell viability was tested using fibroblast cells (L929, BCR, Rio de Janeiro, RJ, Brazil) according to ISO 10993-5. The MTT (3-(4,5-Dimethylthiazol-2-yl)-2,5-Diphenyltetrazolium Bromide) test was performed using polymeric disks (5.0 mm x 1.5 mm²⁰). Three samples from each adhesive group (HEr 0%, 2% and 5%) were sterilized using ethylene oxide

and used to obtain extracts for the test. Cells (L929) were incubated at 37°C in a 5% CO₂ atmosphere and seeded in a 96-well tissue culture plate at a concentration of 10⁴ cells/well (100 µL). The medium consisted of Dulbecco's Modified Eagle's Medium (DMEM, Gibco, Glasgow, UK) supplemented with 10% Fetal Bovine Serum (FBS, Gibco). After 24 hours, the extract was added to each well, and the cells were incubated for 48 and 72 hours at 37°C. For the negative control, the medium was maintained alone. A volume of 50 µL of MTT solution (Invitrogen® CAT No. M6494, 0.005 g MTT, 5 ml PBS, 10 ml DMEM, no FBS) (1 mg/mL) was added to each well. After incubation, the MTT solution was removed, and 200 µL of dimethyl sulfoxide (DMSO) was added to dissolve the formazan crystals. Absorbance was measured at 570 nm (Multiskan EX Microplate Reader, MTX Lab Systems, Vienna, Virginia, USA). Cell viability (expressed as a percentage) for each group was calculated, and the average was determined.

2.7 Statistical analysis

Mineral deposition and cytotoxicity were analyzed descriptively. One-way ANOVA and Tukey's tests were performed for degree of conversion and softening in ethanol. Paired t-tests were used to compare initial and final Knoop microhardness. All tests were conducted at a significance level of 5% using SigmaPlot software.

3. RESULTS

The chemical composition of the hydroxylherderite sample is presented in Table 1, and it matches the ideal formula.

The values for degree of conversion (DC), microhardness, and softening in solvent are in Table 2. No significant changes in DC were observed with the incorporation of hydroxylherderite ($P > .05$). Microhardness values increased significantly ($P < .05$) from 24.30 ± 6.22 (HEr 0%) to 63.21 ± 10.76 after the incorporation of 5% HEr. A significant reduction in microhardness ($P < .05$) was observed after immersion in solvent. The HEr 5% group showed a significant increase in softening in solvent ($81.40 \pm 0.02\%$) compared to the control and HEr 2% groups ($P < .05$).

Mineral deposition was detected on the specimens after seven days of immersion in solution. Phosphate content was not observed on the surface of the control group (HEr 0%) in any time point. A gradual increase in mineral deposition was observed with longer immersion times in the SBF solution and higher HEr concentrations (Figure 1). Different concentrations of HEr maintained cell viability above 80% both 48 hours (Figure 2a) and 72 hours (Figure 2b) of contact.

Table 1. Chemical characterization of hydroxylherderite samples in wt%.

Sample	P ₂ O ₅	MnO	FeO	CaO	Al ₂ O ₃	BeO	F	H ₂ O
Hydroxylherderite	42.57	0.01	0.01	33.89	0.02	15.52	0.07	5.42
Ideal formula ^a	44.06	0.00	0.00	34.82	0.00	15.53	0.00	5.59

^aCalculated on the basis of ideal formula of hydroxylherderite (CaBe(PO₄)(OH)).

Table 2. Degree of conversion (DC) and softening in ethanol ($\Delta\%$) of the adhesive with different concentrations of hydroxylherderite (HEr). DC, in percent (%), initial (KHN1), and final (KHN2) microhardness and softening in ethanol in percent ($\Delta\%$).

Groups	Degree of Conversion	Microhardness		
		Initial	Final	$\Delta\%$
HEr 0%	61.82 \pm 0.79 ^A	24.30 \pm 6.22 ^{Ba}	14.55 \pm 1.76 ^b	37.13 \pm 2.33 ^A
HEr 2%	63.49 \pm 5.30 ^A	19.40 \pm 5.81 ^{Ba}	11.13 \pm 0.21 ^b	39.49 \pm 1.57 ^A
HEr 5%	59.21 \pm 11.11 ^A	63.21 \pm 10.76 ^{Aa}	11.61 \pm 0.68 ^b	81.40 \pm 0.02 ^B

Different upper case indicates significant difference in the same column ($P < .05$).
 Different lowercase indicates a significant difference in the same row ($P < .05$).

UNDER PEER REVIEW

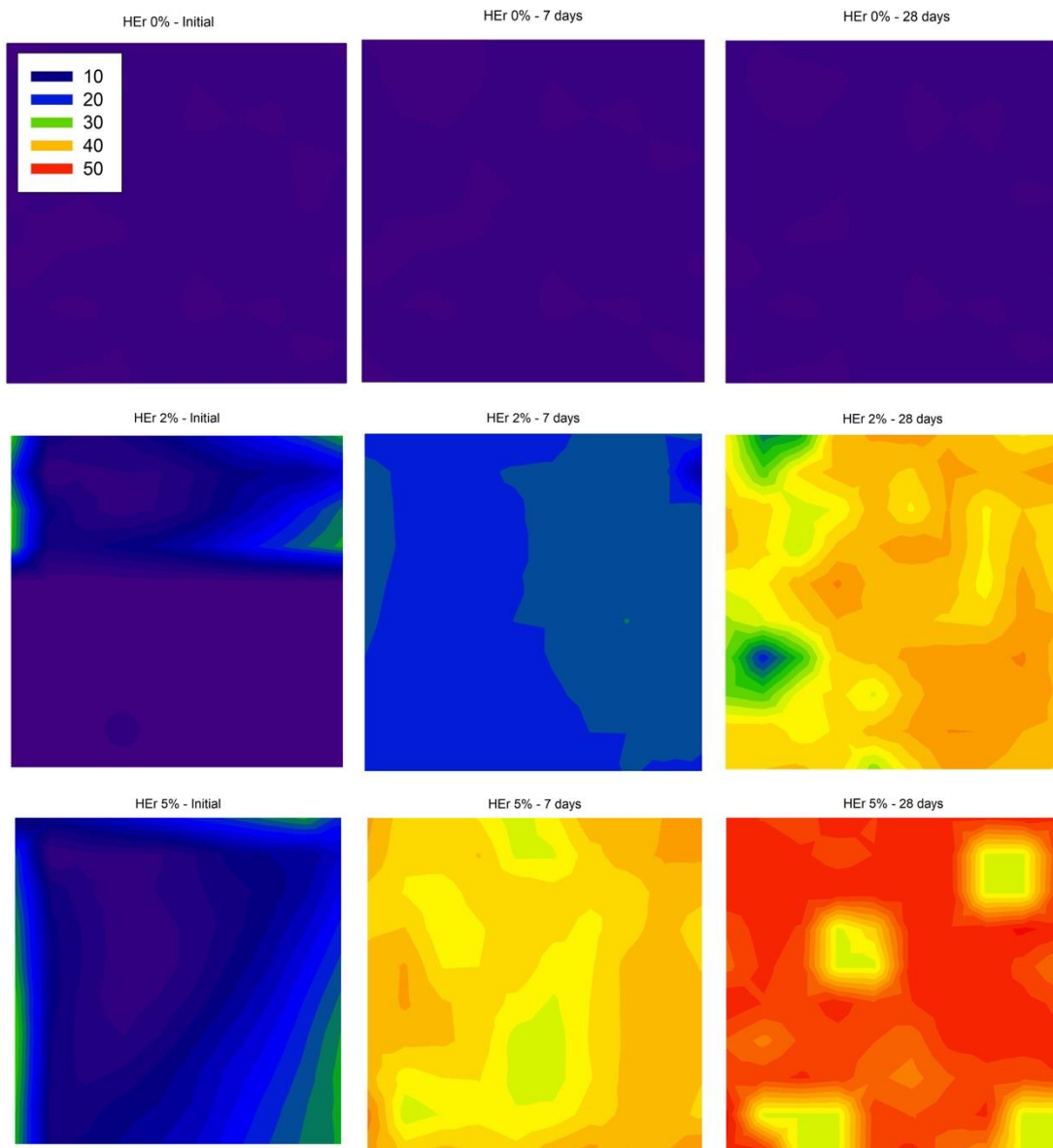


Figure 1. Raman map of phosphate deposition on samples' surface before immersion (initial), after 7 and 28 days of immersion in SBF. The intensity is given by the integration of 960 cm^{-1} peak. The level of mineral deposition intensity is demonstrated according colors scale. HHer 0%: experimental adhesive without addition of hydroxylherderite; HHer 2% and 5%: adhesive containing 2 and 5% of hydroxylherderite.

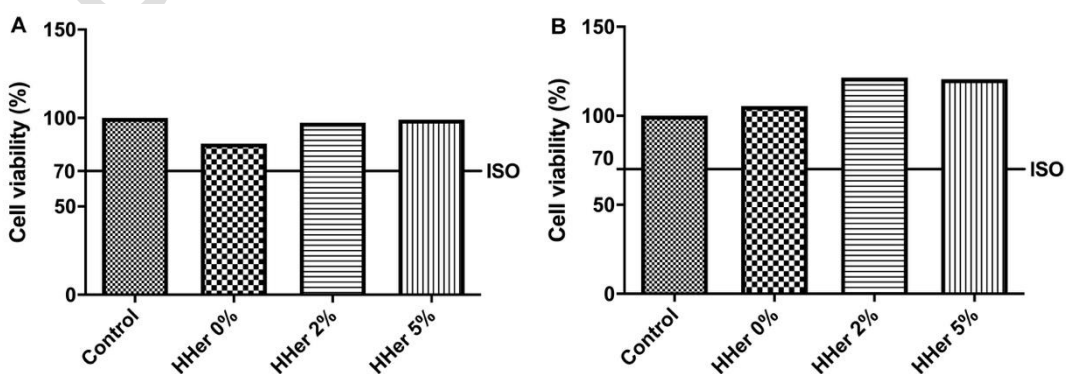


Figure 2. Viable L929 cells (in percent, %), by MTT test, on contact, during 48 h (A) and 72 h (B), to adhesives containing HEr in different concentrations (0%, 2% and 5%) and negative control.

4. DISCUSSION

The remineralization of demineralized dentin is crucial for dentin the long-term stability of dentin bonding²¹. We sought to preserve collagen fibrils within the hybrid layer by incorporating HEr into a conventional adhesive system. HEr is a natural compound from the single-crystal series found in the mid-region of Brazil, recently characterized¹⁴ as containing hard-metal beryllium functionalized with -OH groups. This unique composition suggests that HEr could enhance the adhesive's properties and promote mineral deposition. In this study, the incorporation of Her (at a 2% concentration) promoted mineral deposition, exhibited no cytotoxicity effects, and maintained the adhesive's physicochemical properties.

With a high monomer conversion rate in polymers, fewer unreacted monomers are expected to remain within the polymer matrix²², resulting in improved physicochemical properties of the adhesive. However, excessive incorporation of fillers may hinder light permeation during photoactivation, thereby limiting chains mobility during the propagation phase of polymerization²³. Considering the inorganic composition and size of the fillers, a significant phenomenon of light scattering within the material is plausible^{24,25,26,27}. This scattering effect is further amplified as filler content increases, coupled with a reduction in translucency, which could lead to greater variation in the degree of conversion^{24,25,26,27}. Consequently, this may result in a reduced degree of conversion and compromised mechanical properties of dental adhesives. Notably, the concentrations of HEr used in the present study were adequate to maintain consistent DC values.

Softening in ethanol reflects the crosslink density of the polymer^{3,28}. Solvent uptake and material dissolution occur in the free spaces within the polymer network^{3,28}. The forces of attraction between solvent molecules and polymer chains exceed the forces of attraction between the polymer chains³. The penetration of the solvent leads to the expansion of polymer chain openings³. Polymers with a higher degree of crosslinking are less susceptible to softening, while linear polymers offer more pathways for solvent molecules to diffuse through their structure³. Although an increased degree of conversion (DC) could help preserve the polymer matrix against softening²⁹, polymers with similar DC values may exhibit varying crosslink densities due to differences in chain linearity²⁸. Accordingly, hardness assessment prior to ethanol storage provides an indirect estimation of the degree of conversion³⁰. Meanwhile, the percentage decrease in Knoop hardness following ethanol storage serves as an indicator of the polymer's crosslink density, a critical factor influencing its mechanical properties³¹.

The quality of polymeric matrix of resin-based materials is closely linked to their chemical and thermal stability, which directly influences the longevity of resin restoration³. The methacrylate resin network can be compromised by sorption and solubility effects. The incorporation of inorganic filler particles partially replaces the organic content, thereby providing protection against the deleterious effects of hydrolysis³². The hardness of beryllium, a component of HEr^{13,14}, contributed to the increased microhardness observed in the resin containing 5% of this inorganic compound. However, despite its higher hardness, this property alone was insufficient to prevent material degradation in the solvent. After aging simulation, the resin containing 5% HEr exhibited hardness values comparable to those of other concentrations after aging simulation.

Furthermore, the degradation of materials is influenced by their composition. The presence of calcium, phosphate, hydroxyl groups, and the crystal structure of HEr resembles that of hydroxyapatite (HA). However, while the Ca/P ratio of HA is 1.67, HEr exhibits a Ca/P ratio is 1.0. This ratio is similar to that of monohydrogen calcium phosphates and calcium pyrophosphates, both of which have been utilized in clinical orthopedic and dental applications due to their biomineralization potential³³. Generally, minerals with lower Ca/P ratios tend to exhibit higher solubility³³. The solubility of incorporated HEr may explain why it was unable to prevent polymer degradation.

Rather than preventing solubility, the incorporation of HEr may play a significant role in enhancing mineral availability, potentially benefiting the hybrid layer. Mineral deposition is facilitated by the release of calcium and phosphate ions from resin-based material³⁴. The effect of calcium phosphate compounds involves an initial dissolution process followed by subsequent mineral deposition³⁵, as demonstrated in the images captured at early time points and in previous studies³⁵. Although HEr particles are unable to infiltrate dentinal tubules due to their size, the release of ions can create a supersaturated microenvironment that promotes hydroxyapatite precipitation³⁶. This mineral deposition protects collagen fibrils and can also neutralize acids produced by bacteria, thereby shielding teeth against mineral loss³⁴.

For adhesives containing HEr, phosphate was detected before immersion in simulated body fluid, as Raman spectroscopy identified characteristic bands around 985 and 998 cm^{-1} , corresponding to the stretching vibration of phosphate units¹⁴. Additionally, increasing phosphate and calcium content was observed, proportional to both the HEr concentration and duration of sample immersion in SBF. This confirms that ion release is enhanced by higher phosphate content in the material^{36,37}. Furthermore, it suggests that the mineral deposition capacity of HEr is both cumulative and capable of persisting over time^{36,37}.

To be suitable for application in dental lesions, developed materials must exhibit low toxicity. While resin is commonly used, this study marks the first application of HEr in dental material. The incorporation of HEr maintained cell viability in accordance with ISO 10993-5 recommendations, which require a minimum of 70% cell viability to ensure the biological safety of biomaterials. Furthermore, HEr shares a similar composition with hydroxyapatite, a material known for its lack of cytotoxic effects³⁸. The high cell viability observed confirms that hydroxylherderite holds potential for broad applications in dental materials, including adhesives, composites, sealants, and cements.

The presented study explored two critical aspects of dentin adhesion. The incorporation of fillers tends to reduce hydrolytic effects related to water sorption, which is likely the most significant pathway for bond degradation³⁹. Additionally, biomimetic remineralization promotes both intra- and interfibrillar remineralization, thereby preventing the degradation of exposed collagen³⁹. Although these effects were evaluated, the complexity of the hybrid layer interface-where degradation is linked to both collagen and polymer processes-suggests that longitudinal microtensile bond strength tests of the current material could be a valuable subject for future research.

5. CONCLUSION

It was possible to conclude that hydroxylherderite was successfully incorporated into an adhesive, promoting mineral deposition without cytotoxic effects and maintaining the physicochemical properties of adhesive at a concentration of 2%.

COMPETING INTERESTS DISCLAIMER:

Authors have declared that they have no known competing financial interests OR non-financial interests OR personal relationships that could have appeared to influence the work reported in this paper.

REFERENCES

- 1 Hashimoto M, Tay FR, Svizero NR, de Gee AJ, Feilzer AJ, Sano H. The effects of common errors on sealing ability of total-etch adhesives. *Dent Mater.* 2006;22:560–8.
- 2 Pashley DH, Tay FR, Breschi L, Tjaderhane L, Carvalho RM, Carrilho M, et al. State of the art etch-and-rinse adhesives. *Dent Mater.* 2011;27: 1–16.
- 3 Ferracane JL. Hygroscopic and hydrolytic effects in dental polymer networks. *Dent. Mater.* 2006;22:211–22.
- 4 Breschi L, Mazzoni A, Ruggeri A, Cadenaro M, Di Lenarda R, De Stefano Dorigo E. Dental adhesion review: aging and stability of the bonded interface. *Dent Mater.* 2008;24:90-101.
- 5 Leitune VC, Collares FM, Trommer RM, Andrioli DG, Bergmann CP, Samuel SM. The addition of nanostructured hydroxyapatite to an experimental adhesive resin. *J Dent.* 2013;41:321–7.
- 6 Melo MA, Cheng L, Zhang K, Weir MD, Rodrigues LK, Xu HH. Novel dental adhesives containing nanoparticles of silver and amorphous calcium phosphate. *Dent Mater.* 2013;29(2):199-210.
- 7 Leitune VCB, Schiroky PR, Genari B, Camassola M, S FAL, Samuel SMW, et al. Nanoneedle-like zinc oxide as a filler particle for an experimental adhesive resin. *Indian J Dent Res.* 2019;30(5):777-82.
- 8 Tezvergil-Mutluay A, Seseogullari-Dirihan R, Feitosa VP, Cama G, Brauer DS, Sauro S. Effects of Composites Containing Bioactive Glasses on Demineralized Dentin. *J Dent Res.* 2017;96(9):999–1005.
- 9 Pashley DH, Tay FR, Yiu C, Hashimoto M, Breschi L, Carvalho RM, et al. Collagen degradation by host-derived enzymes during aging. *J Dent Res.* 2004; 83:216–21.
- 10 Kim J, Arola DD, Gu L, Kim YK, Mai S, Liu Y, et al. Functional biomimetic analogs help remineralize apatite-depleted demineralized resin-infiltrated dentin via a bottom–up approach. *Acta Biomater.* 2010;6:2740–50.
- 11 Toledano M, Sauro S, Cabello I, Watson TF, Osorio R. A Zn-doped etch-and-rinse adhesive may improve the mechanical properties and the integrity at the bonded- dentin interface. *Dent. Mater.* 2013;29:e142–52.
- 12 Besinis A, van Noort R, Martin N. Remineralization potential of fully demineralized dentin infiltrated with silica and hydroxyapatite nanoparticles. *Dent. Mater.* 2014;30:249–62.

- 13 Dill HG. The “chessboard” classification scheme of mineral deposits: Mineralogy and geology from aluminum to zirconium. *Earth-Sci Rev.* 2010;100: 1–420.
- 14 Frost RL, Scholz R, López A, Xi Y, Queiroz CS, Belotti FM, et al. Raman, infrared and near-infrared spectroscopic characterization of the herderite–hydroxylherderite mineral series. *Spectrochim Acta A Mol Biomol Spectrosc.* 2014;118:430–7.
- 15 Harlow GE, Hawthorne FC. Herderite from Mogok, Myanmar, and comparison with hydroxyl-herderite from Ehrenfriedersdorf, Germany. *Am Mineral.* 2008;93: 1545–9.
- 16 G.A. Lager, G.V. Gibbs. A refinement of the crystal structure of herderite. *Amer Min.* 1974;59:919–25.
- 17 Mekmene O, quillar S, Rouillon T, Bouler J-B, Piot M, Gaucheron F. Effects of pH and Ca/P molar ratio on the quantity and crystalline structure of calcium phosphates obtained from aqueous solutions. *Dairy Sci Technol.* 2009;89:301–16.
- 18 National Gem Lab. Hydroxylherderite. Accessed 29 November 2024. Available: <https://nationalgemlab.in/hydroxylherderite/>.
- 19 Khan AS, Syed MR. A review of bioceramics-based dental restorative materials. *Dent Mater J.* 2019;31;38(2):163-76.
- 20 Silva EJNL, Herrera DR, Rosa TP, Duque TM, Jacinto RC, Gomes BPFA, Zaia AA. Evaluation of cytotoxicity, antimicrobial activity and physicochemical properties of a calcium aluminate-based endodontic material. *J Appl Oral Sci.* 2014;22(1):61-7
- 21 Degrazia FW, Leitune VCB, Visioli F, Samuel SMW, Collares FM. Long-term stability of dental adhesive incorporated by boron nitride nanotubes. *Dent. Mater.* 2018; 34(3):427-33.
- 22 Collares FM, Ogliari FA, Zanchi CH, Petzhold CL, Piva E, Samuel SMW. Influence of 2-hydroxyethyl methacrylate concentration on polymer network of adhesive resin. *J. Adhes. Dent.* 2011;13:125–9.
- 23 Andrzejewska E. Photoinitiated polymerization of multifunctional monomers. *Polimery.* 2001;46:88–99.
- 24 Arikawa H, Kanie T, Fujii K, Takahashi H, Ban S. Effect of filler properties in composite resins on light transmittance characteristics and color. *Dent Mater J.* 2007;26(1):38-44.
- 25 Salgado VE, Rego GF, Schneider LF, de Moraes RR, Cavalcante LM. Does translucency influence cure efficiency and color stability of resin-based composites? *Dent Mater.* 2018;34(7):957-966.
- 26 Turssi CP, Ferracane JL, Vogel K. Filler features and their effects on wear and degree of conversion of particulate dental resin composites. *Biomaterials.* 2005;26(24):4932-7.

- 27 Lee Y-K. Influence of filler on the difference between the transmitted and reflected colors of experimental resin composites. *Dent Mater.* 2008;24(9):1243-7.
- 28 Schneider LF, Moraes RR, Cavalcante LM, Sinhoreti MA, Correr-Sobrinho L, Consani S. Cross-link density evaluation through softening tests: effect of ethanol concentration. *Dent Mater.* 2008;24:199-203.
- 29 Benetti AR, Asmussen E, Munksgaard EC, Dewaele M, Peutzfeldt A, Leloup G, Devaux J. Softening and elution of monomers in ethanol. *Dent Mater.* 2009;25(8):1007-13.
- 30 Ferracane JL. Correlation between hardness and degree of conversion during the setting reaction of unfilled dental restorative resins. *Dent Mater.* 1985;1:11-4.
- 31 St-Georges AJ, Swift EJ, Thompson JY, Heymann HO. Irradiance effects on the mechanical properties of universal hybrid and flowable hybrid resin composites. *Dent Mater.* 2003;19:406-13.
- 32 Oysaed H, Ruyter IE. Water sorption and filler characteristics of composites for use in posterior teeth. *J Dent Res.* 1986;65(11):1315-8.
- 33 Palmer LC, Newcomb CJ, Kaltz SR, Spoerke ED, Stupp SI. Biomimetic Systems for Hydroxyapatite Mineralization inspired by Bone and Enamel. *Chem Rev.* 2008;108(11):4754-83.
- 34 Braga RR. Calcium phosphates as ion-releasing fillers in restorative resin-based materials. *Dent. Mater.* 2019;35(1):3-14.
- 35 Profeta AC, Mannocci F, Foxton R, Watson TF, Feitosa VP, De Carlo B, Mongiorgi R, Valdré G, Sauro S. Experimental etch-and-rinse adhesives doped with bioactive calcium silicate-based micro-fillers to generate therapeutic resin-dentin interfaces. *Dent. Mater.* 2013;29(7):729-41.
- 36 Aljabo A, Abou Neel EA, Knowles JC, Young AM. Development of dental composites with reactive fillers that promote precipitation of antibacterial-hydroxyapatite layers. *Mater Sci Eng C Mater Biol Appl.* 2016;60:285-92.
- 37 Xu HH, Weir MD, Sun L, Takagi S, Chow LC. Effects of calcium phosphate nanoparticles on Ca-PO₄ composite. *J Dent. Res.* 2007;86(4):378-83.
- 38 Inayat-Hussain SH, Rajab NF, Roslie H, Hussin AA, Ali AM, Annuar BO. Cell death induced by hydroxyapatite on L929 fibroblast cells. *Med. J. Malaysia.* 2004; 59:176-7.

39 Meerbeek BV, Yoshihara K, Van Landuyt K, Yoshida Y, Peumans M. From Buonocore's Pioneering Acid-Etch Technique to Self-Adhering Restoratives. A Status Perspective of Rapidly Advancing Dental Adhesive Technology. Adhes Dent. 2020;22(1):7-34.

UNDER PEER REVIEW